PRAMANA
— journal of
physics

Vol. 65, No. 2
August 2005
pp. 259–272

Role of guard rings in improving the performance of silicon detectors

VIJAY MISHRA*, V D SRIVASTAVA and S K KATARIA
Electronics Division, Bhabha Atomic Research Centre, Trombay, Mumbai 400 085, India
E-mail: eld@magnum.barc.ernet.in; *mishrav@apsara.barc.ernet.in;
mishravijay_73@rediffmail.com

MS received 27 July 2004; revised 1 February 2005; accepted 13 April 2005

Abstract. BARC has developed large-area silicon detectors in collaboration with BEL to be used in the pre-shower detector of the CMS experiment at CERN. The use of floating guard rings (FGR) in improving breakdown voltage and reducing leakage current of silicon detectors is well-known. In the present work, it has been demonstrated that FGRs can also be used to improve the spectroscopic response of silicon detectors. The results have been confirmed by carrying out α-particle ($\approx$5 MeV) and γ-ray (60 keV) spectroscopies with the FGR floating or biased and the underlying physics aspect behind the change in spectra is explained. Although reduction in leakage current after biasing one of the guard rings has been reported earlier, the role of a guard ring in improving the spectroscopic response is reported for the first time. Results of TCAD simulations for silicon detectors with the guard ring under different biasing conditions have been presented. Low yield in producing large-area silicon detectors makes them very costly. However, with one of the FGRs biased even a detector having large surface leakage current can be used to give the same response as a very good detector. This makes the use of large-area silicon detectors very economical as the yield would be very high (>90%).

Keywords. Silicon detectors; floating guard ring; leakage current.

PACS Nos 29.40.Wk; 85.30.Kk; 85.30.De

1. Introduction

Nuclear radiation detectors form the backbone of most of the nuclear physics and high-energy particle physics experiments. Ever since their introduction, semiconductor detectors have been replacing all the conventional nuclear detectors because of their several advantages over traditional detectors. Their compactness and ease of handling have made them popular in nuclear research programs and they also find widespread applications in medicine, space, environment and elemental analysis. The principles of operation of semiconductor detectors is that they are PN junctions which when reverse biased provide charge-depleted regions. When ionizing radiations pass through these regions, they produce free charge carriers. The number of free charge carriers thus produced is proportional to the energy deposited

in the depletion region by the incident radiation. As silicon is extensively used in the microelectronics industry, its material properties and processing techniques are well-studied and best understood. This is why silicon is also the preferred material for fabrication of radiation detectors. Silicon detectors can be fabricated in varied shapes and sizes using standard IC fabrication technology to suit specific applications. Up to now, there are several kinds of high-position resolution silicon detectors, such as silicon drift detectors [1,2], charge coupled devices [3–6], silicon resistive pad detectors [7,8], silicon microstrip detectors [9,10] etc. These detectors are developed using the standard IC fabrication technology. Very recently BARC has developed technology for fabrication of large-area silicon strip detectors in collaboration with BEL, Bangalore [11].

These detectors have been designed with a number of floating guard rings for high-voltage operation of the detectors as it is well-known that high voltage capability of detector diodes fabricated in the planar process is limited by the high field generated at the edge of the junction [12]. An approach to reduce electric field at the junction edges is to use floating guard rings (FGR) which are also P^+ junctions in close proximity to the main junction, surrounding it from all sides but separated from it [13–17].

Besides the conventional application of designing silicon detectors with guard rings, their role in reducing leakage current and improving spectroscopic performance has been investigated in this article. The measurements have been carried out under different biasing conditions of the guard ring for checking the leakage current of detectors when the guard ring is biased or floating. Device simulations have been carried out using MEDICI (a commercial TCAD device simulator tool) in order to understand the underlying device physics explaining the experimental results. Systematic experiments for α-particle and γ-ray spectroscopies have been carried out and the results are presented.

2. Experimental procedure

The detectors have been fabricated using standard silicon planar processing technology. The diodes and strip detector have been fabricated at BEL, Bangalore on $4''$, N-type, $\langle 111 \rangle$, 3–5 kΩ-cm, 300 μm thick silicon wafers from WACKER. Ion implantation has been used for creating P^+/N strips/diodes and for the back N^+ layer. Thermal oxidation has been employed for passivating the silicon surface and for masking during implantation. The metal contact for the front side (32 strips) and back side (common contact for all strips) has been made by evaporating aluminum. The detectors have been passivated using phosphosilicate glass (PSG). The geometry of the strip detector is 60×60 mm^2 which comprises 32 strips with a pitch of 1810 μm. The strip detector is enclosed by seven P^+ guard rings. The single element silicon diode detectors have different areas of 9, 16, 25, 36 and 100 mm^2. These diodes have been put along the periphery of the strip detector. Figure 1 shows the top view of the fabricated $4''$ wafer and a schematic of the cross-section of the peripheral region of diodes and strip detector. The diodes have been designed to have rounded corners and are enclosed in one or two P^+ guard rings. The metal hangover, i.e. metal layer over the oxide extending beyond the P^+ layer

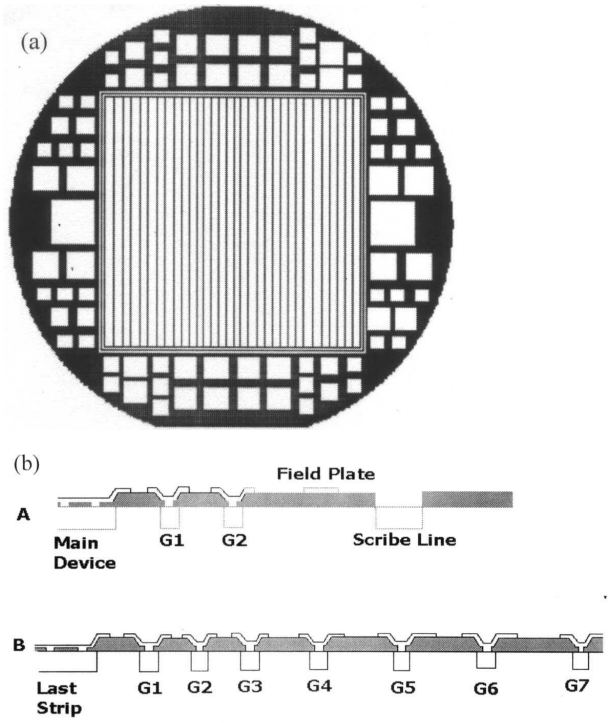

Figure 1. (**a**) Fabricated 4″ wafer showing strip detector of area 6.3 × 6.3 cm^2 and other small area detectors. (**b**) Schematic cross-section of diode detector and strip detector.

has been incorporated for strips and diodes. This technique has been adopted in order to reduce the field at the edge of the junction at the surface. The backside is uniformly N^+ implanted and metallized to create a good ohmic contact. The P^+ and N^+ regions have been obtained by ion implantation and subsequent drive in thermal cycles.

A systematic study has been carried out to understand the role of floating guard rings (FGR) in improving the performance of silicon detectors. The reverse I–V characteristics of the detectors have been measured under different electrical conditions, i.e. guard rings kept floating or biased to the same potential as that of the main diode. Also the I–V characteristics of the guard rings and the main device have been measured simultaneously. The characterization of diodes has been done using a specially made probing arrangement and the I–V characterization set-up developed in BARC was used for simultaneous measurement of leakage current in the main junction and the guard ring. The schematic circuit diagram for the characterization is shown in figure 2. The operational amplifier used for current to voltage conversion is OP128 which has input impedance of 10^{12} Ω [18]. Table 1 lists the leakage current values at different conditions for two detectors of area 9 and 16 mm^2 at a reverse bias of 200 V. The characterization results reveal that leakage current in the main device is significantly reduced by biasing one of the

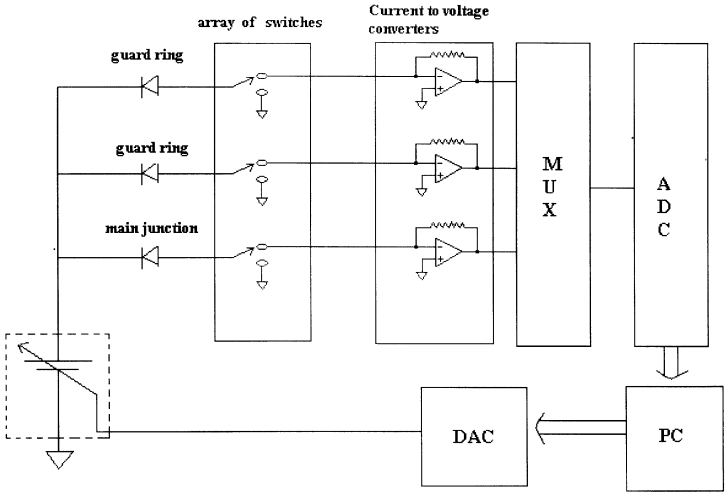

Figure 2. Schematic circuit diagram of the set-up used for the characterization of silicon detectors.

guard rings. This characterization technique was also used to study the effect of grounding the innermost guard ring of a strip detector of geometry 60 × 60 mm^2. The remaining six outer guard rings were kept floating. Figure 3 illustrates that a significant improvement in the I–V characteristics of all the 32 strips of the detector takes place after grounding the guard ring.

The radiation response of the diodes to α-radiation has been evaluated using a ^{241}Am + ^{239}Pu source. The measurements have been performed by keeping the diode and the source in a vacuum chamber maintained at about 10^{-2} Torr. The diodes were reverse biased during measurement and a pre-amplifier (GYNAIC-9413) and shaping amplifier (ORTEC 571) have been used for obtaining the α-spectrum. Figure 4 shows the block diagram of the measurement set-up used for α-particle spectroscopy. The diode detector used for the experiment was a 36 mm^2 area diode. The main junction of the detector is surrounded by a guard ring of width 85 μm. The gap between the main junction and the guard ring is 160 μm. The diode was packaged in a transmission mount so that both the surfaces of the detector were accessible for exposure. Figure 5 shows top view and cross-section of the device used.

Table 1. Leakage current in the main device at different conditions and leakage current in GR for detectors of area 9 mm^2 and 36 mm^2.

	Leakage current through the main device with different conditions at 200 V		Leakage current through the GR at 200 V (nA)
Device	GR floating (nA)	GR grounded (nA)	
9 mm^2	3	1	7
36 mm^2	96	1.6	52

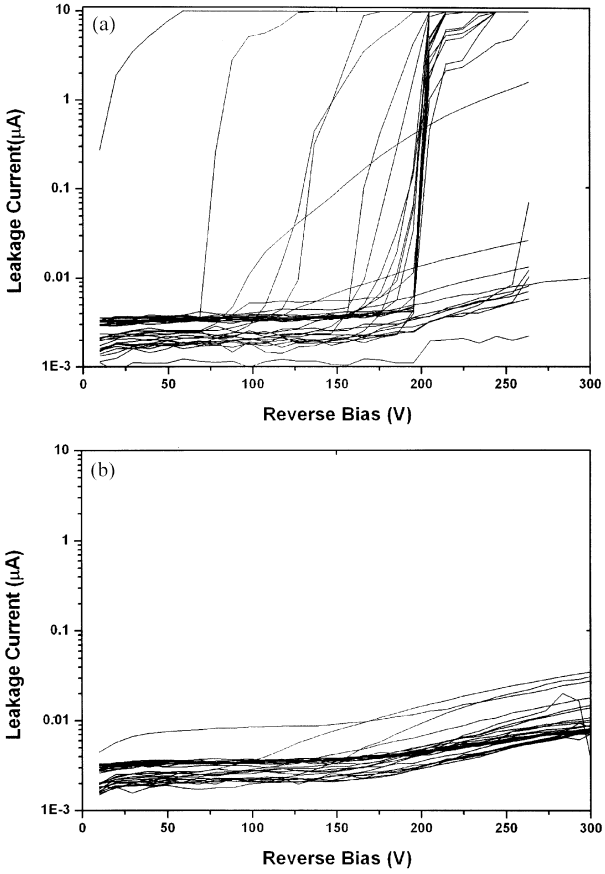

Figure 3. *I–V* characteristics of a 32-strip detector under the conditions of (**a**) guard ring floating and (**b**) guard ring biased.

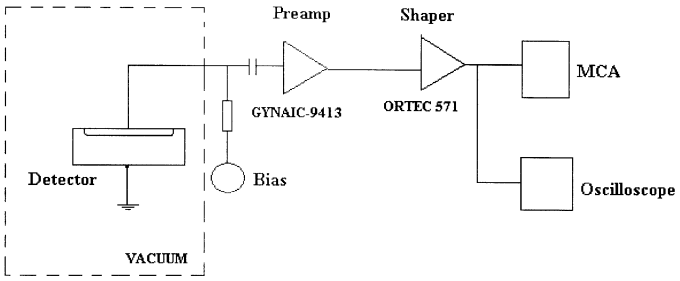

Figure 4. Block diagram of measurement set-up for α-particle spectroscopy.

The α-spectrum was obtained under two electrical conditions with respect to the guard ring. The guard ring was kept floating with no electrical connection to it and an α-spectrum was obtained. The same experiment was repeated with

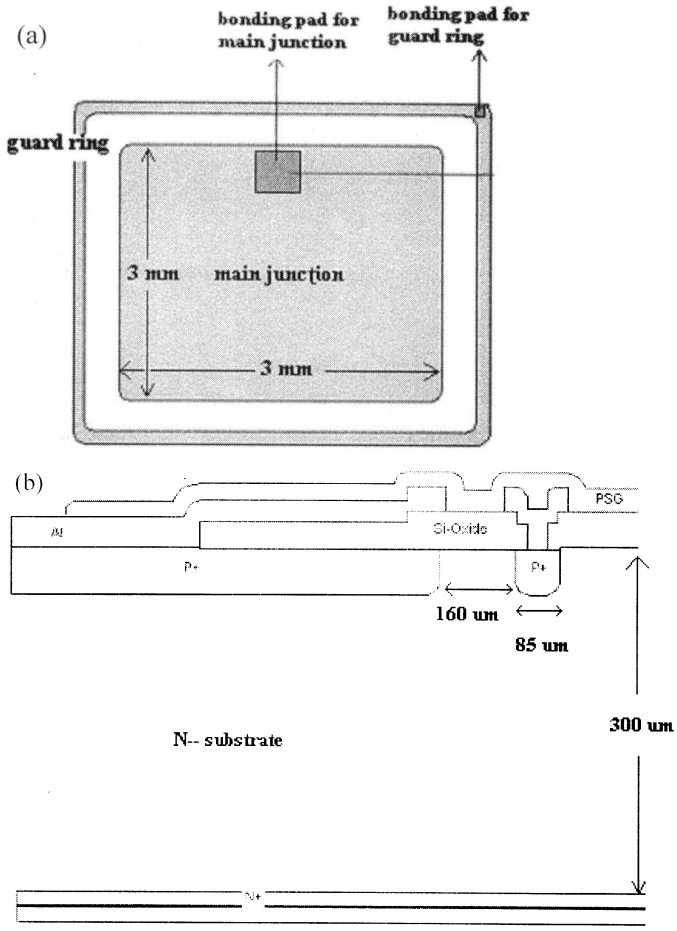

Figure 5. (**a**) Top view and (**b**) cross-sectional view of the 36 mm^2 diode used for α-spectroscopy.

all the experimental conditions the same and the guard ring was biased at ground potential. The response of the diode as an α-detector has been observed to improve after grounding the guard ring. The unexpected peaks A and B appearing in the spectrum with guard ring floating almost completely disappear after grounding the guard ring (figure 6a). This indicates that the extra peaks are formed by the α-particles falling on the guard ring region.

Si-PIN diodes of 9-mm^2 area were packaged in metallic packages at BEL and used to obtain γ-ray spectra. The 60 keV γ-line from ^{241}Am source was recorded on a PC. The reverse bias of 45 V was applied to bias the detector (more than its full depletion voltage). The rise time of the pre-amplifier is around 10 ns and the shaping time was tuned to 2 μs. The γ-spectrum was obtained for the guard ring floating and grounded in a similar fashion as for α-spectroscopy. The energy resolution (FWHM) was found to improve from 3.3 keV to 2.8 keV after grounding

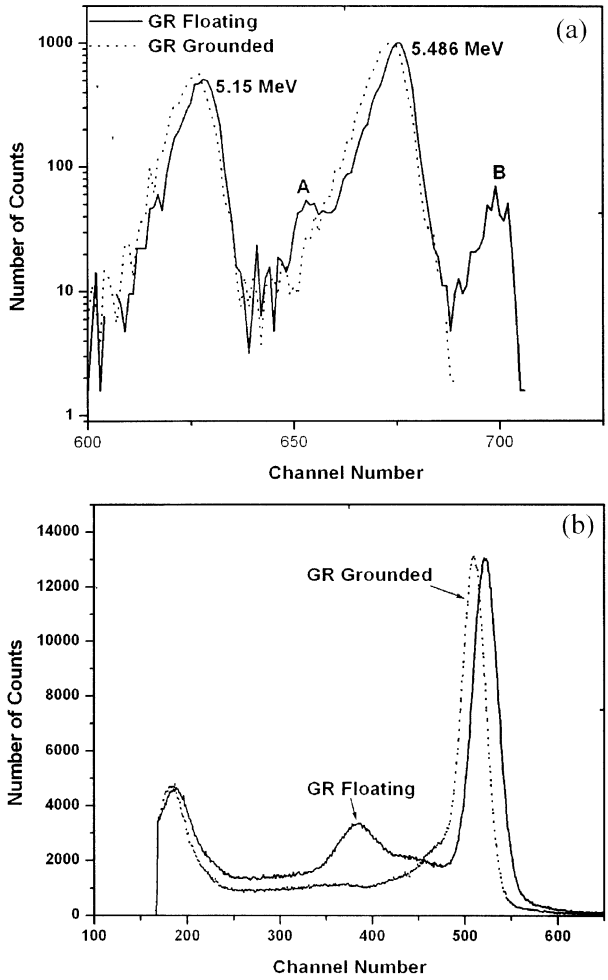

Figure 6. (**a**) Count vs. energy showing a typical γ-ray (60 keV) spectrum under two conditions of guard ring floating and grounded. (**b**) Count vs. channel number showing α-particle spectra for ^{241}Am and ^{239}Pu under the conditions of guard ring floating or grounded, spurious peaks disappear after biasing the guard ring.

the guard ring (figure 6b). The total number of counts in each case is almost equal as both the spectra were taken in the same intervals of time. The spectra were obtained individually and no calibration was carried out.

3. Device simulations

Device simulation using MEDICI was carried out to study the effect of grounding the guard ring on I–V characteristics of the adjacent main junction diode.

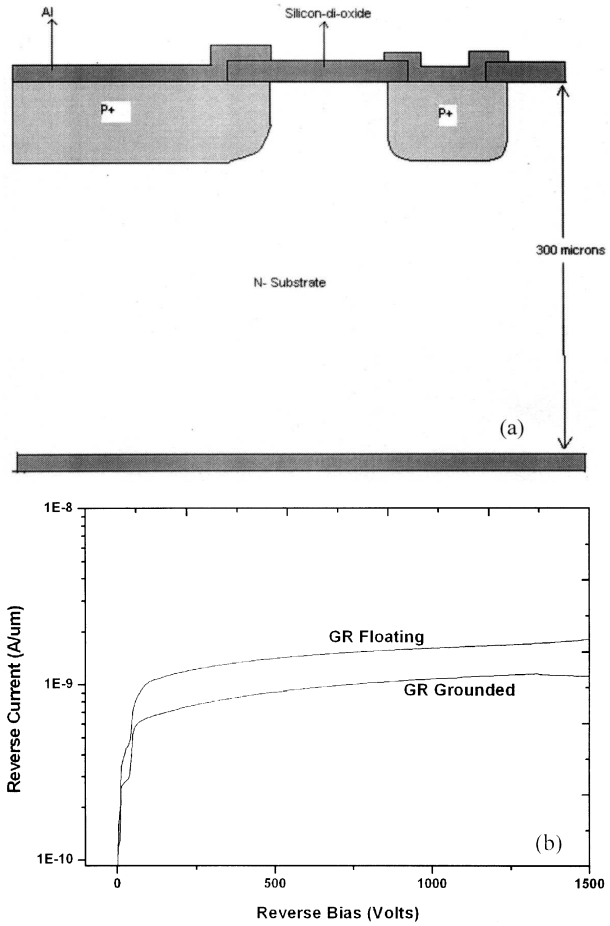

Figure 7. (**a**) Device structure for MEDICI simulations. (**b**) I–V characteristics of the simulated device under different biasing conditions of the guard ring.

Figure 7a shows the cross-section of the simulated device structure. The device is a planar junction of junction depth 3 μm on 300 μm thick high resistivity (1.5×10^{12} cm^{-3}) n-type silicon substrate. The width of the guard ring is chosen to be 50 μm and the gap between the main junction and the guard ring is 30 μm. The oxide thickness is around 1.2 μm. The width of the main junction is 200 μm. The peak doping concentration in the P^+ region is chosen to be 5×10^{19} cm^{-3} with Gaussian distribution.

Figure 7b shows the I–V characteristics of the simulated device with the guard ring floating or grounded. The leakage through guard ring was measured when it was biased to ground potential. The floating configuration of the guard ring was defined by defining the boundary condition at guard ring through which no current flows.

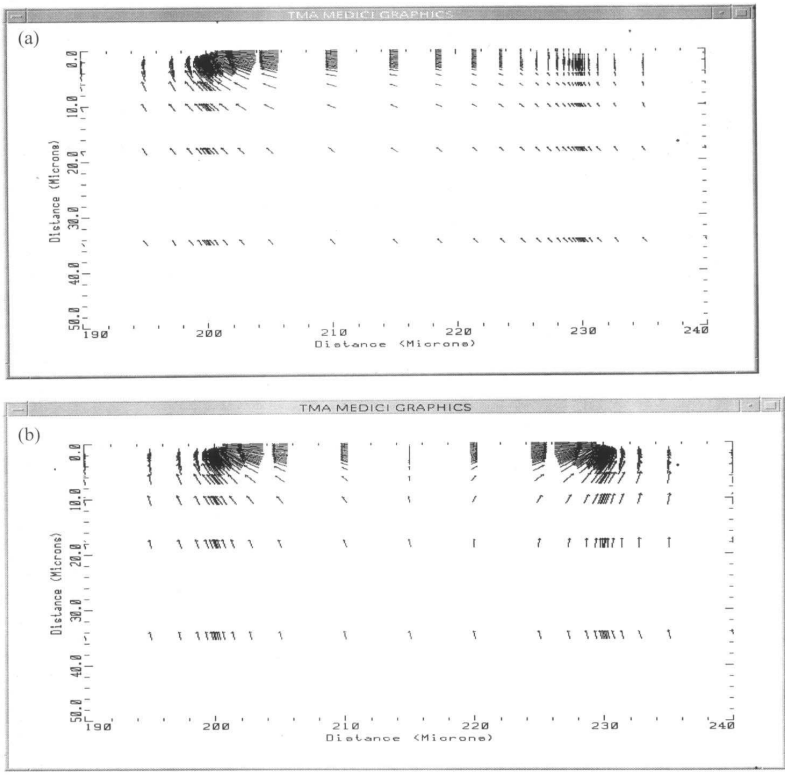

Figure 8. Electric field vectors for the simulated device in the region between main junction and guard ring under the condition of guard ring (**a**) floating and (**b**) biased.

Figures 8a and 8b show the electric field vectors in the region between main junction and guard ring at the surface under two biasing modes of the guard ring, i.e. floating and grounded. The figure depicts that at the device surface, the carriers generated around the guard ring region get collected by the main junction when the guard ring is floating whereas the current generated in the peripheral region (surface as well as bulk components) is collected by the guard ring when it is biased to ground potential. Figure 9 shows the electric field at the surface under the conditions of guard ring floating and biased.

4. Discussions

Table 1 shows that the leakage current in the main diode is significantly reduced with one of the guard rings grounded. The role of guard rings becomes significant when devices are big with large perimeter/area ratio. The larger the perimeter/area ratio for given area area PIN diodes, the higher is the role of surface generated current in total leakage current. Figure 7 shows the simulation result of the diode

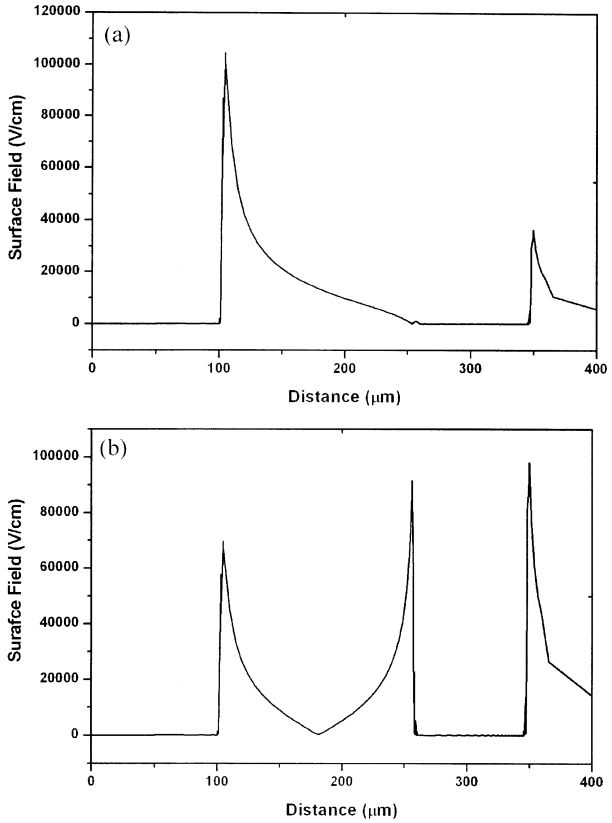

Figure 9. Surface field along the lateral dimension of the simulated structure at reverse bias of 500 V under the condition that guard ring is (**a**) floating or (**b**) biased.

detector. Figure 8 shows the picture of electric current vectors for two separate conditions of guard ring floating and biased. Figure 9 shows the surface field scenario along the length of device for two conditions. The surface field near the main diode is reduced when the guard ring is biased and is increased on the outer side of the guard ring.

The significant advantage of the FGR is confirmed such that in spectroscopic applications, the guard ring collects most of the signal charge generated close to or outside the active area avoiding the number of interactions in which imperfect or incomplete charge collection would occur. We have characterized 36 mm^2 diodes (designed with one guard ring) for 5 MeV α-particles and 9 mm^2 diodes (designed with two guard rings) for 60 keV γ-ray spectra for two different conditions of innermost guard ring floating and biased. Figures 6a and 6b show the results for α-particles and γ-rays respectively. As shown in figures, the spurious peaks adjoining each peak disappear after biasing the guard rings.

Figure 6a shows α-spectra for ^{239}Pu and ^{241}Am sources (5.15 MeV and 5.486 MeV respectively) under two different conditions of guard ring floating and grounded.

The spurious peaks adjacent to each peak disappear after grounding the guard ring. In this case the spurious peaks are on the higher energy side. The α-particles incident on the peripheral region of the detector face less dead layer due to the absence of a P^+ region between the main detector and the guard ring and adjacent peripheral area. Thus α-particles incident on the peripheral region lead to counts on higher energy side. The energy difference between main peaks and respective spurious peaks is in good agreement with the energy deposited by $\approx$5 MeV α-particles in the dead layer absent in the peripheral region. The number of counts of the main peaks and spurious ones are proportional to the main detector area and area of the peripheral region. When the guard ring is biased, the signal charges due to α-particles falling on the peripheral region are collected by the guard ring. The detector was uniformly irradiated to get the spectra for α- and γ-rays.

Figure 6b showing spectrum for 60 keV γ-rays has a spurious peak on lower energy side which disappears after grounding the guard ring. In order to explain these results, figure 10 is drawn to show depletion edges on the periphery of the detector under the two conditions of guard ring floating (edge A) and grounded (edge B) and full depletion voltage applied at backside ohmic contact. The peripheral region of the detector is only partially depleted ($\approx$150 μm) when the guard ring is kept floating. When X-ray photons are absorbed in the non-depleted region of the detector substrate below the guard ring and adjacent area, the generated carriers move towards the electrodes by the diffusion mechanism and only partially get collected to the electrodes. Therefore, such incidents lead to counts on the low-energy side. This is supported by the fact that the number of counts in the 60 keV peak and spurious peak are proportional to the main detector area and the peripheral region consisting of the guard ring. When the guard ring is biased, the depletion edge changes its shape (edge B) and the detector substrate below the peripheral region is fully depleted which avoids the incidents of incomplete charge collection. Also there is improvement in energy resolution due to reduced value of leakage current after grounding the guard ring. The leakage current of the PIN diode used for obtaining γ-spectra is reduced from 3 nA to 1 nA after grounding the guard ring.

For a PN junction detector, reverse bias capacitance is given by eq. (1).

$$C_j = \frac{A}{2}\left[\frac{2q\varepsilon_{\mathrm{Si}}}{V_0 - V}N_{\mathrm{d}}\right]^{1/2}, \tag{1}$$

where A is the area of the detector, q is the electronic charge, $\varepsilon_{\mathrm{Si}}$ is the permittivity of silicon and N_{d} is the density of donor atoms. Calculation of the detector capacitance at reverse bias of 45 V gives a value of 4.165 pF. This value would increase by 17% after grounding the guard ring with 17% increase in effective area of junction. The slight shift in peak after biasing the FGR is attributed to change in output capacitance of the detector.

Achieving a good yield in detector manufacturing is difficult due to the requirement of maintaining high-quality semiconductor properties during high temperature processing, the need of processing both sides of wafer and the large area of silicon detectors approaching the size of the wafers. Although we have achieved a yield of 50% in producing the strip detectors of area 6.0 $\times$ 6.0 cm^2 and later 6.3 $\times$ 6.3 cm^2, there is a significant number of detectors with one or two strips showing high surface leakage current. The detectors with even one strip showing leakage current

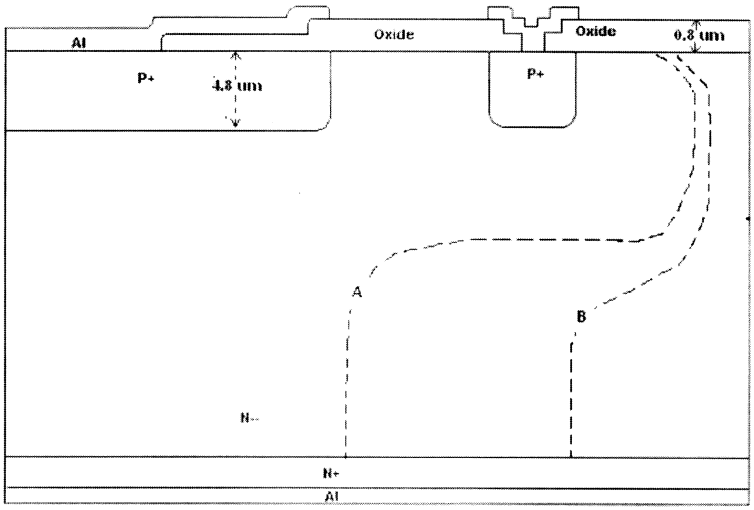

Figure 10. Depletion edges on the periphery of the detector under two conditions of guard ring floating (edge A) and grounded (edge B) and more than full depletion voltage applied at backside ohmic contact.

more than 1 μA of current do not qualify due to the specifications set by the preshower group of CERN. The study of leakage current of detectors with guard ring floating or biased has revealed that the surface component of the leakage current can be substantially reduced by biasing one of the guard rings to the same potential as the main diode. Figure 3a shows the leakage current in all 32 strips of a detector of area 6.0 $\times$ 6.0 cm^2 with all the FGRs floating and figure 3b shows the change in I–V characteristics after biasing the innermost FGR. Simulations indicate that when the guard ring is grounded, it collects most of the surface-generated current. Three PIN diodes of exactly same area with varying perimeters and fabricated on the same silicon wafer showed reverse leakage current values which are dependent on the perimeter extent. This gives evidence that (a) the current is indeed surface generated and (b) the surface current is the dominant contribution to the overall leakage current. When the guard ring of the diodes is grounded, the leakage current values become closely equal [19]. This result is consistent on several samples on different wafers fabricated in a batch. Also the devices have always been sawn at designed scribe lines of width 50 μm at a spacing of 280 μm from the device edge. The region of scribe line is implanted with phosphorous with dose 5×10^{15} at 80 keV and devoid of SiO_2. The depletion edge would be far from the sawn edge at reverse bias voltage of 45 V. It is proposed that the strip detectors that show high surface leakage current in strips can become usable detectors with one of the guard rings grounded. Under the FGR floating condition, the innermost guard ring gets biased by the punch-through mechanism and in the presence of even a minute surface region with a large number of surface states huge current flows between P^+ strips and N^-substrate. When the innermost FGR is externally biased to the same potential as that of strips, no current flows between the two and the surface component of the leakage current is collected through the guard ring. Leakage current

in the small area diodes (9 mm^2, 16 mm^2, 25 mm^2 and 100 mm^2) fabricated on the peripheral region of the wafers also reduced after biasing the guard rings. While producing large-area strip detectors at BEL, a yield of 50% has been achieved as per qualifying specifications by CERN. Thus large numbers of strip detectors with one or two strips exceeding a leakage current of 1 μA at reverse bias of 300 V are produced and considered to be rejected. These detectors with one of the FGRs biased are excellent quality large-area strip detectors that can be used in physics experiments. The yield of producing large-area strip detectors increases up to 90% or even higher when strip detectors are used with one of the FGRs biased.

5. Conclusions

Large-area silicon detectors have been designed and fabricated with guard ring structures. A systematic study has been carried out to explore the role of guard rings in improving the performance of silicon detectors with emphasis on reducing leakage current and improving the spectroscopic performance. The added advantage of floating guard ring in reducing leakage current and improving the spectroscopic response of silicon detectors has been studied and reported. Device simulations have been done which match with the experimental results. The low yield in producing large area silicon detectors which makes them very costly can be overcome by using them with one of the floating guard rings biased. The large-area silicon strip detectors have low yield (around 50%) which makes them very costly. With one of the guard rings biased during operation, the leakage current of the strips reduces significantly and their electrical characteristics are as good as good detectors.

Acknowledgements

The authors want to convey their deep gratitude to J Vasi, R Lal and Dinesh Sharma of IIT, Bombay for their fruitful suggestions during the development programme of silicon detectors and providing computation facilities for carrying out the study. The authors are thankful to Prabhakar Rao and Shankarnarayana of BEL, Bangalore for carrying out fabrication of detectors. The authors would like to thank Anita Topkar, V B Chandratre and M Y Dixit for the useful discussions during this study. The authors are thankful to D Sahoo for his help in alpha spectroscopy measurements and A K Mohanty for discussions and support.

References

[1] E Gatti *et al*, *Nucl. Instrum. Methods* **226**, 129 (1984)
[2] Pavel Rehak *et al*, *Nucl. Instrum. Methods* **A248**, 376 (1986)
[3] R Bailey *et al*, *Nucl. Instrum. Methods* **A213**, 201 (1983)
[4] Mario Bocciolini *et al*, *Nucl. Instrum. Methods* **A240**, 36 (1985)
[5] L Struder *et al*, *Nucl. Instrum. Methods* **A257**, 594 (1987)
[6] J Alcaraz *et al*, *Nucl. Instrum. Methods* **A284**, 303 (1989)

[7] S J Alvsvaag *et al*, *IEEE Trans. Nucl. Sci.* **42**, 469 (1995)
[8] E Laegsaard *et al*, *Nucl. Instrum. Methods* **A60**, 24 (1968)
[9] P Weilhammer, *Nucl. Instrum. Methods* **A324**, 1 (1994)
[10] G F Dalla Betta *et al*, *Nucl. Instrum. Methods* **A460**, 306 (2001)
[11] Vijay Mishra *et al*, *Nucl. Instrum. Methods* **A527**, 308 (2004)
[12] S M Sze and G Gibbons, *Solid State Electron.* **9**, 831 (1966)
[13] K P Brieger *et al*, *Solid State Electron.* **26**, 739 (1983)
[14] M S Adler *et al*, *IEEE Trans. Electron Devices* **ED-24**, 107 (1977)
[15] S K Ghandi, *Semiconductor power devices* (Wiley, New York, 1977)
[16] Lars Evensen *et al*, *Nucl. Instrum. Methods* **A337**, 44 (1993)
[17] M Da Rold *et al*, *IEEE Trans. Nucl. Sci.* **46**, 1215 (1999)
[18] A Das *et al*, Automated and multi-channel characterization systems for silicon strip detectors, in the *Proceedings of Symposium on Intelligent Nuclear Instrumentation* (BARC, February 2001) pp. 236–241
[19] Vijay Mishra, *Study of silicon detectors*, PhD thesis (Mumbai University, December 2002)